Acta Pharmaceutica Sinica B 2024;14(8):3591−3604

Chinese Pharmaceutical Association
Institute of Materia Medica, Chinese Academy of Medical Sciences

Acta Pharmaceutica Sinica B

www.elsevier.com/locate/apsb
www.sciencedirect.com

ORIGINAL ARTICLE

Inhibition of xanthine oxidase alleviated pancreatic necrosis *via* HIF-1α-regulated LDHA and NLRP3 signaling pathway in acute pancreatitis

Juan Rong [a,b,†], Chenxia Han [a,†], Yan Huang [a,†], Yiqin Wang [a], Qi Qiu [a], Manjiangcuo Wang [b,c], Shisheng Wang [d], Rui Wang [c], Juqin Yang [e], Xia Li [f,g], Chenggong Hu [g], Zhiyao Chen [a], Lihui Deng [a], Wei Huang [a,e], Qing Xia [a,*], Dan Du [a,b,c,d,*]

[a]*West China Center of Excellence for Pancreatitis, Institute of Integrated Traditional Chinese and Western Medicine, West China Hospital/West China Medical School, Sichuan University, Chengdu 610041, China*
[b]*State Key Laboratory of Bioactive Substance and Function of Natural Medicines, Institute of Materia Medica, Chinese Academy of Medical Sciences and Peking Union Medical College, Beijing 100050, China*
[c]*Advanced Mass Spectrometry Center, Research Core Facility, Frontiers Science Center for Disease-related Molecular Network, West China Hospital, Sichuan University, Chengdu 610213, China*
[d]*Proteomics-Metabolomics Platform, Research Core Facility, Institutes for Systems Genetics, West China Hospital, Sichuan University, Chengdu 610093, China*
[e]*Biobank, West China Hospital, Sichuan University, Chengdu 610093, China*
[f]*West China School of Nursing, Sichuan University, Chengdu 610041, China*
[g]*Department of Critical Care Medicine, West China Hospital, Sichuan University, Chengdu 610041, China*

Received 11 November 2023; received in revised form 6 February 2024; accepted 15 March 2024

KEY WORDS

Xanthine oxidase inhibitor;
Multi-omics;
HIF-1α;

Abstract Acute pancreatitis (AP) is a potentially fatal condition with no targeted treatment options. Although inhibiting xanthine oxidase (XO) in the treatment of AP has been studied in several experimental models and clinical trials, whether XO is a target of AP and what its the main mechanism of action is remains unclear. Here, we aimed to re-evaluate whether XO is a target aggravating AP other than merely generating reactive oxygen species that trigger AP. We first revealed that XO expression and

*Corresponding authors.
E-mail addresses: dudan1520@163.com (Dan Du), xiaqing@medmail.com.cn (Qing Xia).
†These authors made equal contributions to this work.
Peer review under the responsibility of Chinese Pharmaceutical Association and Institute of Materia Medica, Chinese Academy of Medical Sciences.

https://doi.org/10.1016/j.apsb.2024.04.019

Necrotizing acute pancreatitis;
Lactate;
Therapeutic target;
NLRP3;
Metabolic flux

enzyme activity were significantly elevated in the serum and pancreas of necrotizing AP models. We also found that allopurinol and febuxostat, as purine-like and non-purine XO inhibitors, respectively, exhibited protective effects against pancreatic acinar cell death *in vitro* and pancreatic damage *in vivo* at different doses and treatment time points. Moreover, we observed that conditional *Xdh* overexpression aggravated pancreatic necrosis and severity. Further mechanism analysis showed that XO inhibition restored the hypoxia-inducible factor 1-alpha (HIF-1α)-regulated lactate dehydrogenase A (LDHA) and NOD-like receptor family pyrin domain containing 3 (NLRP3) signaling pathways and reduced the enrichment of $^{13}C_6$-glucose to $^{13}C_3$-lactate. Lastly, we observed that clinical circulatory XO activity was significantly elevated in severe cases and correlated with C-reactive protein levels, while pancreatic XO and urate were also increased in severe AP patients. These results together indicated that proper inhibition of XO might be a promising therapeutic strategy for alleviating pancreatic necrosis and preventing progression of severe AP by downregulating HIF-1α-mediated LDHA and NLRP3 signaling pathways.

1. Introduction

Acute pancreatitis (AP) is characterized by inflammation of the exocrine pancreas, primarily caused by gallstones, alcohol, and hypertriglyceridemia[1,2]. While most cases of AP are mild, approximately 20%−30% progress to a severe form[3]. Pancreatic necrosis[4,5] occurs in 20%−40% of severe AP (SAP) cases, often accompanied by worsening organ failure, and the mortality rates are 35.2% and 19.8% for infected and sterile necrosis, respectively[6]. Current treatments for SAP involve antibiotic therapy, surgical interventions, and supportive care, but there is a lack of drugs with well-defined targets[3,7,8]. Although numerous chemical agents or drugs have been tested in clinical trials, their promising benefits have yet to be demonstrated[9].

Xanthine oxidase (XO) was previously proposed as a drug target in early AP[10]. It was implicated as the main source of reactive oxygen species (ROS) in pancreatic acinar cells (PACs) when irreversible conversion from xanthine dehydrogenase (XDH) catalyzed by trypsin or chymotrypsin and reversible conversion by thiol group oxidation[10,11]. Nevertheless, prophylactic administrations of allopurinol (ALLO), a purine-like XO inhibitor (XOI)[12], to prevent early ROS generation have not achieved consistent efficacy in various experimental AP[10,13-16] and endoscopic retrograde cholangiopancreatography (ERCP) induced AP[17-21]. Instead, therapeutic administrations of XOIs have been proven to show benefits in several necrotizing AP animal models[22-26]. Therefore, administration with XOIs during SAP progression at the proper time point and concentration might be an effective route to re-evaluate their therapeutic value.

Moreover, there is growing evidence that XO plays a significant role in escalating local inflammation and systemic damage. Once XO activation occurs, the XO form catalyzes monovalent and divalent electron transfer to O_2, resulting in superoxide ions and hydrogen peroxide (H_2O_2)[27]. It is well known that ROS-induced oxidative stress mediates the mitogen-activated protein kinase signaling pathway in the pancreas[25], and aggravates damage to the lung and kidney[16,23]. However, whether the excessive consumption of O_2 even leads to hypoxia during ROS production is not clear. It has been reported that XO could regulate the activation of hypoxia-inducible factor 1-alpha (HIF-1α) in other diseases[28]. Both hypoxia[29] and upregulation of HIF-1α escalated inflammation and metabolic disturbance during pancreatitis[30,31]. Thus, it is necessary to investigate the metabolic and inflammatory impact of XO activation accompanied by hypoxia on disease progression.

In this study, we compared the XO enzyme activity and expressions of XO gene and protein in animal models and PACs of varying severity. We also evaluated the therapeutical efficacy of two kinds of XOIs and the exacerbation effect of conditional overexpression of *Xdh* in necrotizing AP models and studied the downstream metabolic pathways and inflammatory signaling pathways using multi-omics, metabolic flux, and other biochemistry approaches. Lastly, we detected XO and its metabolite expressions in plasma and *in situ* tissue from SAP patients. Altogether, we sought to (1) evaluate the therapeutical doses and effects of XOIs in alleviating pancreatic necrosis in SAP and (2) explore the action mechanism of XO in addition to merely generating ROS.

2. Material and methods

A detailed description of the Materials and Methods for Reagents and Antibodies (Supporting Information Table S1), Isolation of PACs and *in vitro* Studies, Biochemical Assays, Histology, Immunohistochemistry (IHC), and Immunofluorescence, Western-blot (WB) and Real Time-quantitative Polymerase Chain Reaction (RT-qPCR), RNAscope *in situ* Hybridization, Mass Spectrometry Imaging, RNA Sequencing Analysis, Targeted Metabolomics, Bioinformatic Analysis, Molecular Docking, Cell Metabolic Flux Analysis, and Cellular Thermal Shift Assay can be found in the Supporting Information Materials and Methods.

2.1. Animals and experimental models

Male C57BL/6J mice and Sprague−Dawley rats were purchased from Beijing Huafukang Biotechnology Co., Ltd. or Jiangsu Gempharmatech Co., Ltd. The animals were housed at a temperature of 21 ± 2 °C with a 12-h light−dark cycle and provided with a standard laboratory chow diet and *ad libitum* access to food and water. All animal experiments were conducted following the approved protocols of the Animal Ethics Committee of West

China Hospital, Sichuan University (approval numbers: 2020 321A; 20220315007).

Three AP models were employed: (1) Six to eight-week-old male mice ($n > 6$) weighing ~22 g received 7 hourly intraperitoneal injections of 50 μg/kg cerulein to induce a mild edematous model of AP (CER-AP). (2) Eight to ten-week-old male mice ($n > 10$) weighing ~25 g received two intraperitoneal injections of 4 g/kg L-arginine (ARG, 8.8%, pH = 7.0) at a 1-h interval to induce a severe necrotizing AP (ARG-AP). (3) Eight to ten-week-old rats ($n > 5$) weighing ~230 g received retrograde pancreatic ductal injection of 5% sodium taurocholate (NaT, 1 mL/kg) to induce severe biliary AP (NaT-AP). Control groups received intraperitoneal injections of 0.9% sodium chloride saline at the same volume, or control rats underwent a sham operation without NaT perfusion.

For treatment with XOIs, mice were (1) intraperitoneally injected with 30 mg/kg ALLO starting from 8 h and twice a day for the next two days; (2) intraperitoneally injected with 2 and 10 mg/kg febuxostat (FEB) twice a day starting from 8 h; and (3) intraperitoneally injected with 0.5, 2, and 10 mg/kg FEB at 48 and 56 h. Rats received intragastric gavage of 20 mg/kg ALLO at 0.5 and 4 h after surgery. Model groups received the same volume of solvent as treatment groups.

For adenovirus-mediated overexpression, adenoviruses expressing *Xdh* and control green fluorescent protein were obtained from Vigene Bioscience (Jinan, China). Adenovirus was administrated to the pancreas using an intraductal infusion system following a previously established protocol[32]. Briefly, six to eight-week-old male mice received retrograde pancreatic ductal injection of adenoviruses at a concentration of 2.2×10^9 plaque-forming units/mL. Mice were infected with adenoviruses for 7 days before ARG-AP model establishment, dead mice were excluded. The efficiency of infection was assessed using fluorescence microscopy and RT-qPCR analysis (Supporting Information Table S2).

Animals were sacrificed at designated time points after the first injection. Serum was collected for the measurement of amylase, lipase, glutathione peroxidase (GPx), superoxide dismutase (SOD) enzyme activities, aspartate aminotransferase, urea, and creatinine. The entire pancreas was immediately excised. Separated pancreas samples were used for trypsin and myeloperoxidase (MPO) activity measurement, XO enzyme activity measurement, histopathological assessment, and Western blot or RT-qPCR analysis. Lung sections were also isolated for MPO and histopathological analysis. Tissues used for histological assessment were fixed in 10% formalin for paraffin embedding. Serum and pancreatic tissues used for biochemical and omics studies were aliquoted, shock-frozen in liquid nitrogen, and stored at −80 °C.

2.2. Cell culture and transfection

The mouse-derived PAC line 266-6 was obtained from the American Type Tissue Collection (ATCC, Rockville, MD, USA). Cells were cultured in Dulbecco's modified Eagle's medium supplemented with 10% heat-inactivated fetal bovine serum and 1% penicillin and streptomycin at 37 °C, 95% humidity, and 5% CO_2. Small interfering RNAs (siRNA) targeting *Xdh* or a scrambled siRNA were constructed by Tsingke Biotechnology Co., Ltd. (Beijing, China). Cells were seeded at a density of 1.0×10^5 cells per well in a 12-well plate for 24 h before transfection. The indicated siRNA (50 nmol/L) was transfected into 266-6 cells at 60%−80% confluence using a Lipofectamine 3000 Transfection Reagent following the manufacturer's protocol.

2.3. Human studies and samples collections

All human studies adhered to the principles outlined in the Declaration of Helsinki and received approval from the Institutional Review Board and Biomedical Ethics Committee of West China Hospital, Sichuan University (approval numbers: 2017, no. 456; 2020, no. 196). Written informed consent was obtained from all patients before blood and/or pancreatic tissue sampling. Biobanking procedures, clinical data collection, and storage followed our previous study[33].

The inclusion and exclusion criteria were reported in our previous study[34]. Briefly, inclusion criteria were: (1) age, 18−75 years old; (2) meet the diagnostic criteria of the AP[35]; (3) admitted to the hospital within 48 h of onset. Pregnancy, cancer, and major infectious diseases were excluded. The AP severity of patients was categorized as mild (no local or systemic complications), moderately severe (local complications without persistent organ failure), and severe (persistent organ failure regardless of local complications) by the revised Atlanta classification[35] and 2018 American Gastroenterological Association Guidelines[8]. Peripheral venous blood samples were collected from AP patients within 72 h after the onset of abdominal pain. Blood was collected in ethylenediaminetetraacetic acid tubes for plasma determination, following our established protocol[33,36]. Plasma samples from fasting healthy volunteers (HV) were obtained from the West China Biobanks. Control pancreatic tissue samples were obtained from patients who underwent left-sided or small unobstructed pancreatic tumor resection, following a previous protocol[37]. SAP pancreatic tissue samples were obtained from patients undergoing necrosectomy, including necrotized and adjacent inflamed pancreata. Written informed consent was obtained from the patients or their legal guardians. All the clinical data for patients is noted in Supporting Information Tables S3−S5.

2.4. Statistical analysis

All data are presented as mean ± standard error of the mean (SEM). Statistical analysis was performed using GraphPad Prism 8.0.1 software (La Jolla, CA, USA). Data from two groups were analyzed using an unpaired two-tailed Student's *t*-test or Mann−Whitney U test. Data from multiple groups were analyzed using one-way ANOVA with Dunnett's multiple comparison tests or non-parametric tests with the Kruskal−Wallis H test. Categorical data of clinical samples were reported as numbers with percentages and were compared using a chi-square test. A *P*-value of less than 0.05 was considered statistically significant.

3. Results

3.1. Enzyme activity, mRNA, and protein expressions of XO were significantly increased in necrotizing AP

In the ARG-AP mice, pancreatic necrosis and inflammation were observed at 48 and 72 h after the first ARG injection (Fig. 1A and B). Serum XO activity increased as early as 8 h after the first injection (Fig. 1C) and continued to rise until 72 h. The mRNA expression of *Xdh* increased immediately at 8 h and peaked at 72 h with an average fold increase of 40 (Fig. 1D), which was

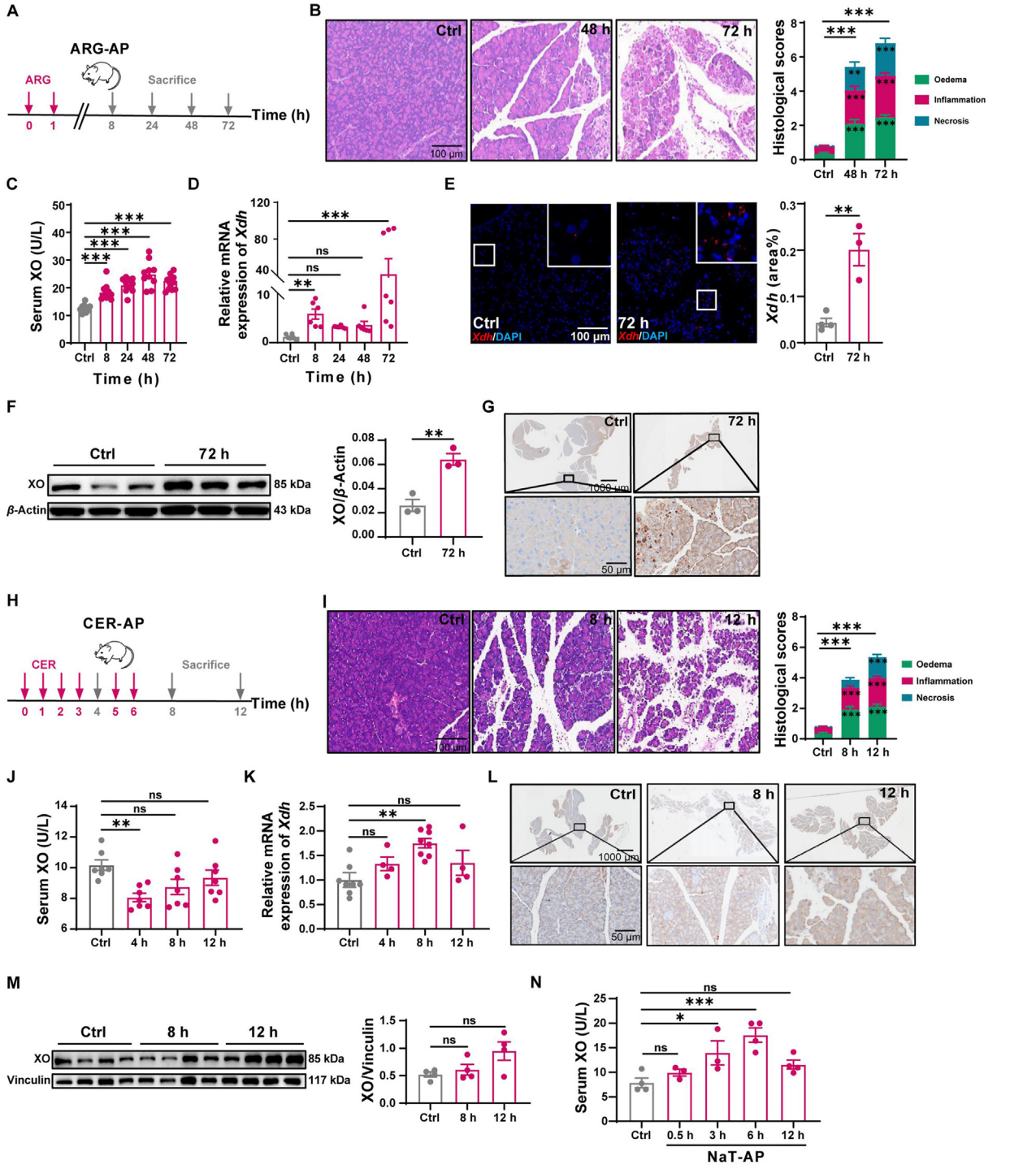

Figure 1 XO was significantly increased in necrotizing AP. (A) The schematic diagram of ARG-AP modeling. (B) Representative hematoxylin and eosin (H&E) pancreas images with stacked histological scores of ARG-AP mice ($n = 6-11$) ($^{**}P < 0.01$, $^{***}P < 0.001$ *vs.* Ctrl). (C) Serum XO activity of ARG-AP mice ($n = 10-11$). (D) Relative mRNA expression of *Xdh* in the pancreas of ARG-AP groups ($n = 6-7$). (E) *In situ* RNA scope of pancreatic *Xdh* expression in ARG-AP at 72 h ($n = 3-4$). (F) WB assay of pancreatic XO expression and quantitative result on ARG-AP mice at 72 h ($n = 3$). (G) Representative images of IHC for pancreatic XO expression at 72 h. (H) The schematic representation of CER-AP modeling. (I) Representative H&E pancreas images with stacked histological scores of CER-AP mice ($n = 6-8$) ($^{***}P < 0.001$ *vs.* Ctrl). (J) Serum XO activity of CER-AP mice ($n = 7$). (K) Relative mRNA expressions of *Xdh* in the pancreas of CER-AP groups ($n = 4-8$). (L) Representative images of IHC for pancreatic XO expression at 8 and 12 h in CER-AP mice. (M) WB assay of pancreatic XO expression and the quantitative result of CER-AP mice ($n = 4$). (N) Serum XO activity of NaT-AP rats at different time points ($n = 3-4$). Data are presented as mean ± standard error of the mean (SEM); ns means no significance, $^{*}P < 0.05$, $^{**}P < 0.01$, and $^{***}P < 0.001$.

consistent with the *in situ* gene expression of *Xdh* at 72 h (Fig. 1E). Correspondingly, pancreatic XO protein expression was three times higher in the 72-h group compared to the control group (Fig. 1F and G). In the edematous CER-AP mice, pancreatic edema, inflammation, and scattered necrosis were observed at 8 and 12 h after the first cerulein injection (Fig. 1H and I). No significant increase in serum XO activity was observed in CER-AP (Fig. 1J). The *Xdh* mRNA expression increased at 4, 8, and 12 h and achieved significance at 8 h compared to the control group (Fig. 1K). Pancreatic XO protein levels at 8 and 12 h had an increased propensity compared to the control group, according to IHC and WB data (Fig. 1L and M). Additionally, serum XO activity in the NaT-AP rat model was increased as early as 3 h after modeling (Fig. 1N). *In vitro*, cell toxins including cerulein, taurolithocholic acid 3-sulfate disodium salt (TLCS), H_2O_2, and ARG were found to increase XO protein expression in PACs (Supporting Information Fig. S1A), and the enzyme activities of XO were significantly increased after H_2O_2, ARG, and TLCS stimulation with a serial concentration gradient as well as hypoxia and hypoxia plus 500 μmol/L TLCS (Fig. S1B). Meanwhile, hypoxia plus TLCS aggravated PACs necrosis in comparison to applying them alone (Fig. S1C). These data suggest that XO was significantly increased in both peripheral circulation and pancreas in severe necrotizing AP models, while it was slightly increased in the edematous model, demonstrating the potential role of XO in SAP.

3.2. *XO inhibitors significantly improved severe necrotizing AP in vitro and in vivo*

ALLO and FEB[12] can inhibit XO through XO−XOI hydrogen bond interactions, as demonstrated by computer simulation (Fig. 2A and Supporting Information Fig. S2A). Both ALLO and FEB demonstrated a dose-dependent protective effect against TLCS, hypoxia, and TLCS plus hypoxia-induced cell death (Fig. 2B, Fig. S2B and S2C). Furthermore, the inhibitory effect of XO enzyme activity sensitized by H_2O_2, ARG, TLCS, hypoxia, and TLCS plus hypoxia was further confirmed in ALLO and FEB treatments (Fig. 2C and Fig. S2D). As expected, 180 μmol/L ALLO significantly reduced H_2O_2-induced ROS, with *N*-acetylcysteine used as a positive control for ROS content (Fig. 2D). Additionally, a cellular thermal shift assay was performed to

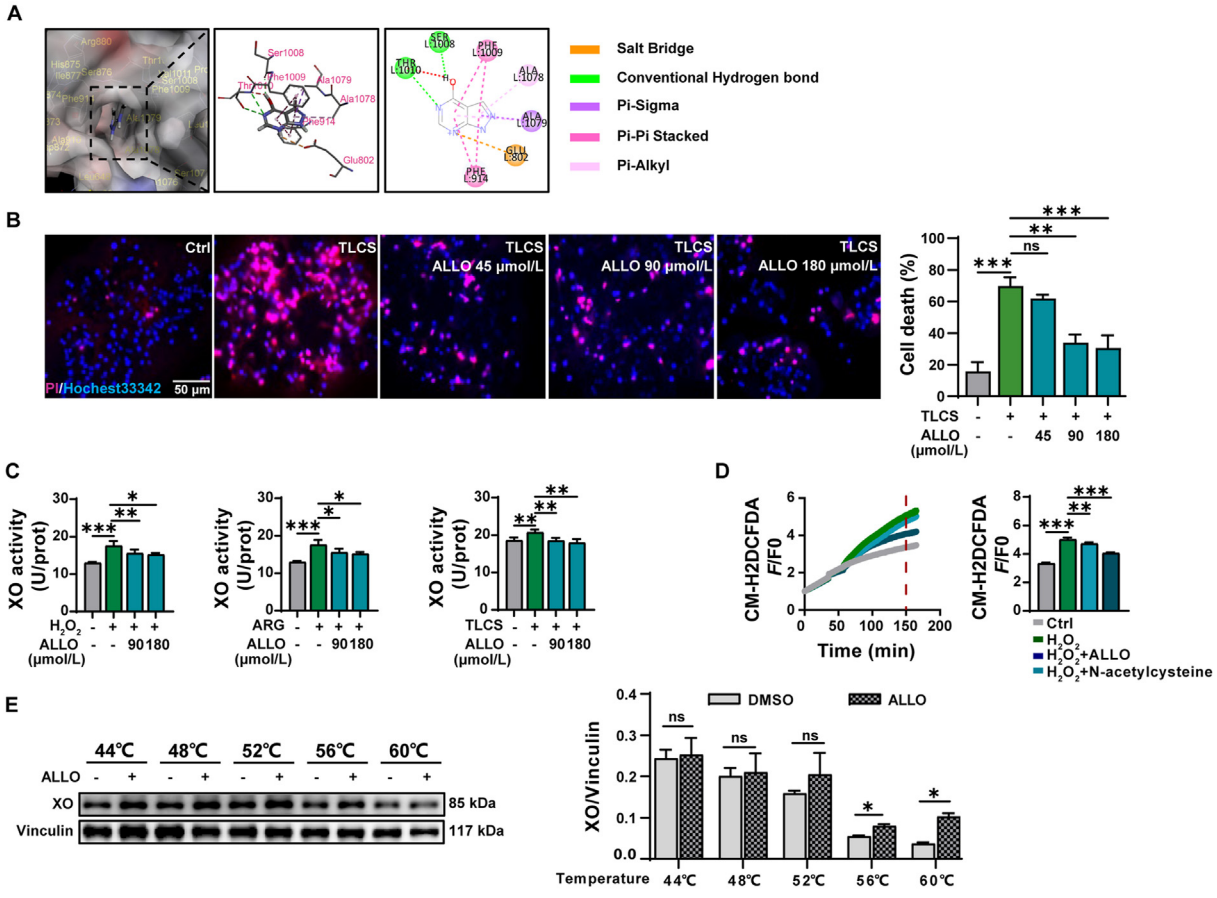

Figure 2 Inhibition of XO protected against cell death in PACs. (A) Molecular docking of ALLO binding to XO. Two hydrogen bonds were indicated in ALLO-Thr1010 and ALLO-Ser1008. (B) Representative images and quantitative results for ALLO protections on TLCS-induced PACs death ($n = 3$). (C) XO activation occurred by stimulation of H_2O_2 (100 μmol/L), ARG (100 mmol/L), and TLCS (100 μmol/L), and was inhibited by ALLO ($n = 3$). (D) Protective effects of ALLO (180 μmol/L) on ROS generation induced by H_2O_2 (100 μmol/L) on PACs, *N*-acetylcysteine was used as a positive control, and quantitative results among four groups at 150 min are presented ($n = 3$). (E) ALLO (1 mmol/L) treatment significantly increased the thermal stability between XO and PACs at 56 and 60 °C ($n = 3$). Data are presented as mean ± SEM; ns means no significance, $^*P < 0.05$, $^{**}P < 0.01$, and $^{***}P < 0.001$.

investigate the stability of XO and ALLO interactions in PACs. As expected, 180 μmol/L ALLO increased the thermal stability of XO in PACs, with rising temperatures reaching statistical significance at 56 and 60 °C (Fig. 2E).

The effects of ALLO and FEB administrations on experimental necrotizing AP were investigated. A schematic diagram of ALLO administration is presented in Fig. 3A. ALLO at 30 mg/kg administered from 8 h significantly decreased pancreatic necrosis

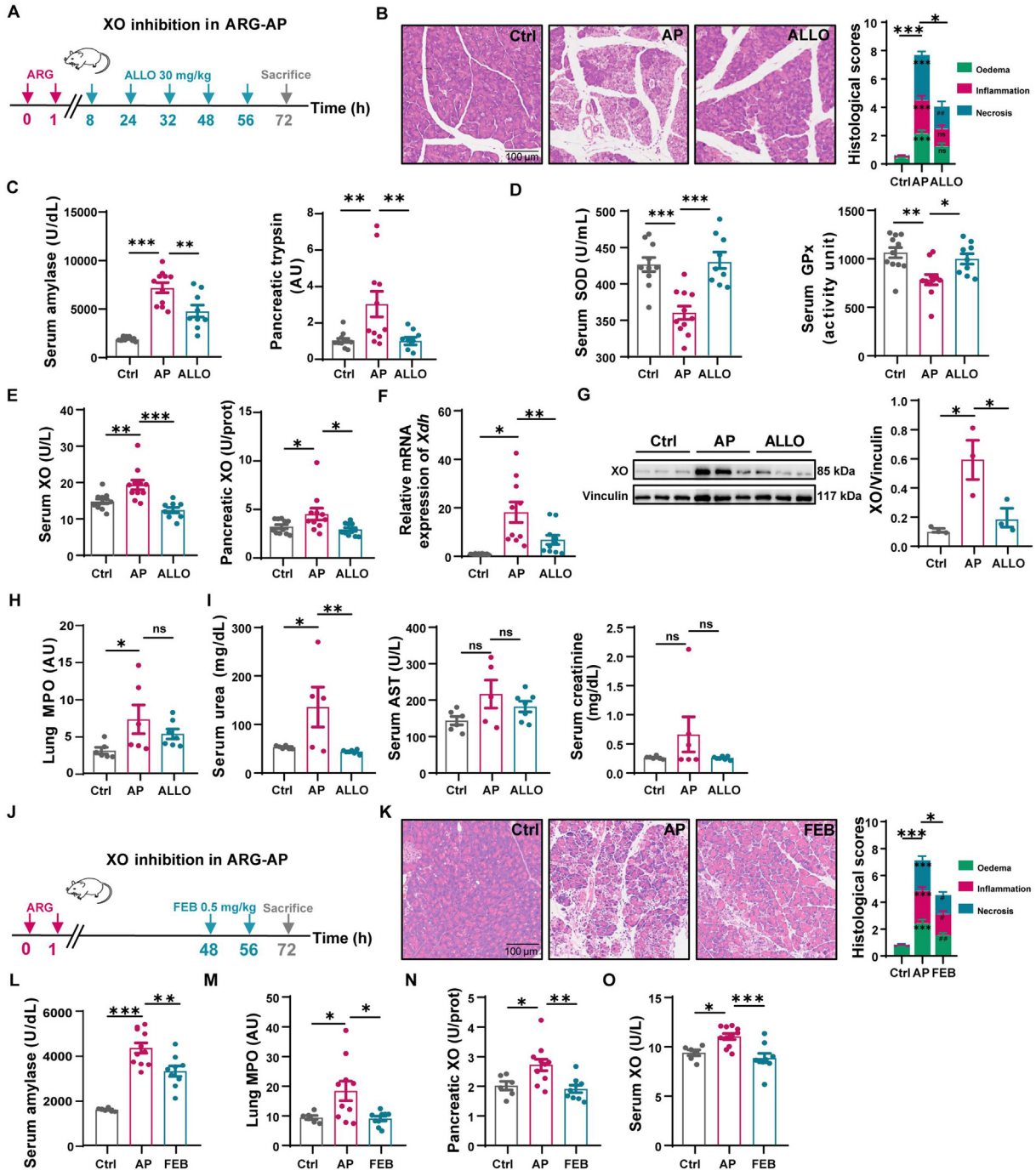

Figure 3 Inhibition of XO significantly ameliorated disease severity in ARG-AP. (A) Schematic representation of ARG injections and ALLO administrations. (B) Representative H&E pancreas images with stacked histological scores (n = 9−12; $^{***}P < 0.001$ *vs.* Ctrl, $^{\#\#}P < 0.01$ *vs.* AP). (C) Serum amylase and pancreatic trypsin activity (n = 9−12). (D) Serum SOD (n = 9−11) and GPx activity (n = 9−12). (E) Serum and pancreatic XO activity (n = 9−12). (F) Relative mRNA expression of X*dh* in pancreas (n = 10−12). (G) WB analysis of pancreatic XO expression and quantitative results (n = 3). (H) Lung MPO (n = 6−7). (I) Serum urea (n = 5−7), aspartate aminotransferase (AST) (n = 5−7), and creatinine levels (n = 6−7). (J) Schematic representation of ARG injections and FEB administrations. (K) Representative H&E pancreas images with stacked histological scores (n = 6−11; $^{***}P < 0.001$ *vs.* Ctrl, $^{\#}P < 0.05$, $^{\#\#}P < 0.01$ *vs.* AP). (L) Serum amylase (n = 6−11) (M) Lung MPO (n = 6−10). (N) Pancreatic XO activity (n = 6−11). (O) Serum XO activity (n = 6−11). Data are presented as mean ± SEM; ns means no significance, $^{*}P < 0.05$, $^{**}P < 0.01$, and $^{***}P < 0.001$.

(Fig. 3B), serum amylase, and pancreatic trypsin activity (Fig. 3C), as well as increased systemic oxidative stress markers, including serum SOD and GPx levels (Fig. 3D). Analysis of XO enzyme activity in serum and pancreas (Fig. 3E), along with XO gene and protein expressions (Fig. 3F and G), further confirmed the therapeutic efficacy of ALLO. Parameters of distant organs, including lung MPO levels (Fig. 3H) and circulative levels of urea, creatinine, and aspartate aminotransferase (Fig. 3I), were reduced in the ALLO treatment group compared to the AP group, with urea reaching significance. However, FEB administered from 48 h showed a better improvement in reducing parameters than that from 8 h (Supporting Information Fig. S3). FEB at 0.5 mg/kg (Fig. 3J) significantly reduced pancreatic necrosis (Fig. 3K), serum amylase levels (Fig. 3L), lung MPO levels (Fig. 3M), pancreatic XO (Fig. 3N), and serum XO levels (Fig. 3O). The effect of ALLO at 20 mg/kg in NaT-AP rats was also evaluated. ALLO significantly reduced disease severity assessments, including pancreatic histological damage (Supporting Information Fig. S4A and S4B), serum amylase level (Fig. S4C), and serum XO level (Fig. S4D), as well as increased SOD and GPx activities (Fig. S4E). These data together suggest that the blockade of XO ameliorates SAP by using different kinds of XOIs at proper concentrations and time points.

3.3. Multi-omics analysis reveals HIF-1α-regulated LDHA and NOD-like receptor family pyrin domain containing 3 (NLRP3) signaling pathways play important roles in inhibiting XO

To explore the mechanism of XO inhibition, RNA sequencing was performed. Volcano plots (Fig. 4A) and Venn analysis (Fig. 4B) revealed 101 overlapped distinct genes, and their expressions were shown in a heatmap combined with a violin plot (Supporting Information Fig. S5A). Gene ontology and Kyoto Encyclopedia of Genes and Genomes (KEGG) analysis were then conducted. The primary gene ontology terms were displayed in a variant chord plot (Fig. S5B and Table S6). The top 21 enriched KEGG pathways are shown in Fig. 4C and Supporting Information Table S7, with NOD-like receptor signaling pathways (mmu04621) and HIF-1α signaling pathway (mmu04066) enriched with the metabolic gene *Ldha*. Accordingly, pancreatic mRNA levels of *Hif1a*, *Ldha, Nlrp3*, *Il1b*, and *Caspase-1* (*Casp1*) (Fig. 4D), as well as protein levels of HIF-1α and LDHA (Fig. 4E), were increased in AP and reversed by XOI treatment. Given that XO and HIF-1α participate in purine metabolism and glycolysis metabolism, respectively (Fig. 4F), targeted metabolomics was performed to measure the relative abundance of corresponding metabolites. A Pearson correlation analysis between urate and other metabolites indicated that lactate was the most relevant metabolite to urate ($R^2 = 0.9128$ for AP *vs*. control in Fig. 4G, and $R^2 = 0.873$ for ALLO *vs*. AP in Fig. 4H). The abundance of metabolites from glycolysis, including lactate, pyruvate, glucose, and glucose-6-phosphate, was significantly enhanced in the AP group. Lactate and urate were significantly reduced after ALLO treatment (Fig. 4I). Additionally, the ratio of pyruvate/phosphoenolpyruvic acid increased in AP and decreased in the ALLO group, as did the ratio of urate/hypoxanthine (Fig. 4J). Taken together, XO inhibition affects the NLRP3 and HIF-1α signaling pathways, as well as anaerobic glycolysis and purine catabolism.

3.4. Pancreatic overexpression of Xdh aggravated AP severity and upregulated downstream HIF-1α signaling pathway

Conditional pancreatic *Xdh* overexpression in mice was established using the adenovirus infusion system (Fig. 5A), which emits a unique overexpression of *Xdh* marked with green fluorescence (Fig. 5B). After ARG injection, a higher mortality (37.5%) was observed in the adenovirus-*Xdh* overexpressing AP group *vs*. wide type (WT)-AP group (12.5%). Compared with the WT-AP group, there was an evident increase in serum lipase, pancreatic trypsin, and pancreatic necrosis in adenovirus-*Xdh* overexpressing AP mice (Fig. 5C−F). The oxidative damage was also significantly increased after *Xdh* overexpression, evidenced by pancreatic ROS (Fig. 5G), serum SOD and GPx level (Fig. 5H). These were most likely due to an elevation in serum XO enzyme activity (Fig. 5I), pancreatic *Xdh* gene (Fig. 5J), and XO protein (Fig. 5K). Additionally, pancreatic HIF-1α and LDHA protein showed an increase in adenovirus-*Xdh* overexpressing AP mice compared with the WT-AP group (Fig. 5K), along with the downstream genes including *Hif1a*, *Nlrp3*, *Il1b*, and *Casp1* (Fig. 5L). These results demonstrate that pancreatic XO overexpression may aggravate pancreatic injury during AP *via* activating HIF-1α.

3.5. Inhibition of XO downregulated HIF-1α-mediated LDHA and NLRP3 signaling pathways

Next, we used a PAC line to investigate the effect of *Xdh* gene deletion. The mRNA of *Hif1a* and *Ldha* showed a relative decrease after the knockdown of the *Xdh* gene by siRNA transfection in 266-6 cell lines (Supporting Information Fig. S6). Then, a time-dependent increase in mRNA expressions of *Xdh* and *Hif1a* was observed in hypoxia-treated primary PACs (Fig. 6A) and ARG-AP pancreas (Fig. 6B), indicating the prioritized order of *Xdh*. XOIs were then employed on PACs under hypoxia, resulting in decreased mRNA expression of *Hif1a*, *Ldha*, *Nlrp3*, *IL1b*, and *Casp1*(Fig. 6C and Supporting Information Fig. S7). Furthermore, a reversal of protein expressions of HIF-1α and LDHA was observed after ALLO treatment in PACs (Fig. 6D and E). Additionally, the labeled ratio of metabolites in glycolysis and the tricarboxylic acid cycle from $^{13}C_6$-glucose in PACs were traced (Fig. 6F). As suggested in Fig. 6G, under hypoxic conditions, the M+3 labeling lactate level was significantly increased. ALLO reduced the buildup of labeled lactate, with no effect on aerobic metabolism. Finally, the HIF-1α inhibitor PX-478 (Fig. 6H) was used in PACs and found to improve cell death induced by TLCS (Fig. 6I) and decrease mRNA levels of the *Ldha* and *Nlrp3* pathways (Fig. 6J). However, HIF-1α inhibition did not reverse *Xdh* mRNA expression (Fig. 6K) or XO activity (Fig. 6L). Together with the prior data, these results suggest that inhibition of XO decreased HIF-1α-mediated LDHA and NLRP3 signaling pathways.

3.6. Increased circulative and pancreatic XO was found in patients with severe AP

A brief protocol for human sample detection is shown in Fig. 7A. We examined the XO activity in plasma from HV and AP patients of different severity. XO activity was considerably higher in SAP patients than in HV, mild AP (MAP), and moderately severe AP (MSAP) patients, respectively (Fig. 7B). C-reactive protein, a marker used to predict the severity of AP, showed a higher correlation coefficient between XO and C-reactive protein in non-MAP (MSAP + SAP) patients compared to MAP patients (Fig. 7C). Pancreatic tissues were collected from SAP patients. The *in situ* mRNA (Fig. 7D) and protein expressions (Fig. 7E) of XO, as well as the catabolite urate of XO (Fig. 7F), were measured

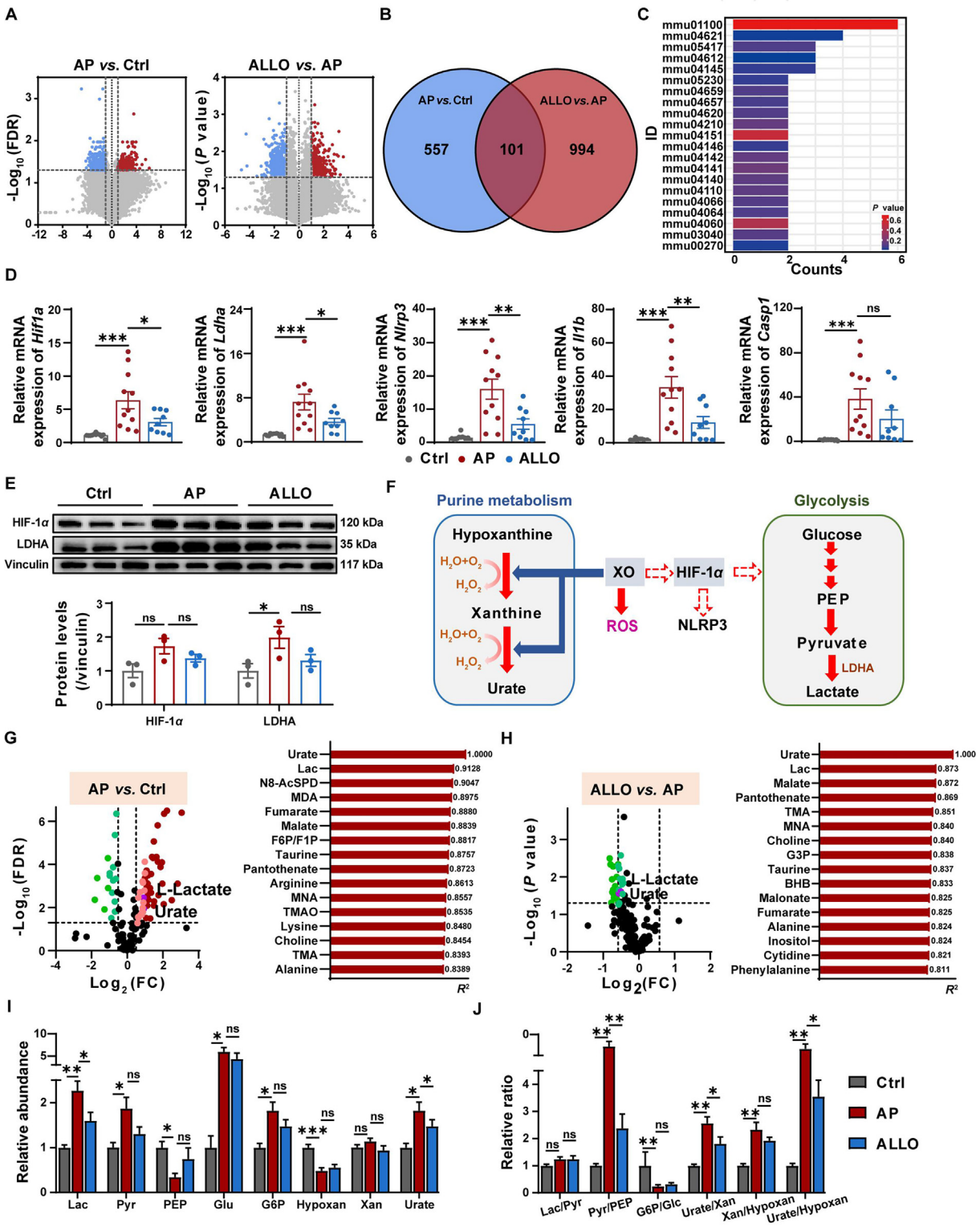

Figure 4 Inhibition of XO affected HIF-1α-regulated LDHA and NLRP3 signaling pathways in ARG-AP. (A) The volcano plots (left) of identified genes for AP *vs*. Ctrl and ALLO *vs*. AP groups, with significantly down-regulated genes (blue), up-regulated genes (red), and non-significant genes (grey), with the Log_2FC of different gene expression on the *x*-axis and the statistical significance on the *y*-axis ($n = 4$). (B) Venn diagram displayed 101 overlapped (middle) objects (FC > 1.5 or < 0.67 and FDR <0.05 for AP *vs*. Ctrl; FC > 1.5 or <0.67 and $P < 0.05$ for AP *vs*. ALLO) between each two groups. (C) Top 21 pathways of KEGG analysis (Table S7). (D) Relative mRNA expressions of *Hif1a*, *Ldha*, *Nlrp3*, *Il1b*, and *Casp1* in Ctrl, AP, and ALLO groups in ARG-AP ($n = 9–12$). (E) WB analysis of pancreatic HIF-1α and LDHA ($n = 3$). (F) Schematic diagram of the role of XO and HIF-1α in purine metabolism and glycolysis. Dotted red arrows indicated assumed relationships. (G) The volcano plot (left) of identified metabolites for AP *vs*. Ctrl (green dots for 2 times down-regulation, blue dots for 1.5 times down-regulation,

to confirm the XO alteration in the necrotic pancreas. The *in situ* gene expression of *XDH*, co-labeled with amylase, was significantly higher in SAP than that in the control group, along with increased protein expression and ion intensity of urate. Furthermore, we compared clinical data on the plasma levels of LDH and lactate in AP patients of various severities up to admission and found higher contents of LDHA and lactate in the SAP group (Fig. 7G) than those in MAP. The toxicity of different doses of lactate on PACs was preliminarily determined, indicating that a high concentration of lactate significantly induced cell death (Supporting Information Fig. S8). These clinical data indicate that levels of XO are related to the severity of AP and also suggest that peripheral expressions of XO and lactate are necessary to predict the progression of AP.

4. Discussion

The pathogenetic theories and risk factors associated with SAP are still a subject of mystery, despite numerous attempts to investigate the potential targets aggravating the disease[2,38]. During the past 30 years, although some preliminary studies have been conducted on the efficacy of inhibiting XO in AP, it is unclear whether XO is a target for AP and the main mechanism other than ROS involved in amplifying inflammatory disease. For instance, most of the previous experimental studies pretreated with XOIs in AP models did not work on all the AP models[10,13-16], but therapeutical dosing has yielded benefits in some necrotizing models[22,23,26]. The administration dose of XOIs is also different in each study. Additionally, prophylactic administration of ALLO at various doses did not yield consistent benefits in ERCP-induced AP in previous random controlled trials[17-21]. The main reasons may be related to the sample size, simplex etiology, disease severity, and improper concentration and administration methods. Therefore, we aim to evaluate the therapeutical doses and effects of XOIs in alleviating pancreatic necrosis in SAP and explore its main downstream mechanism based on animal models, primary cell models, and severe patient-related data.

In this study, we first employed three experimental AP models with varying levels of severity and identified XO enzyme activities and expressions that were exclusively increased in necrotizing ARG-AP or NAT-AP, but not significant in the edematous AP model. These are consistent with earlier reports that ROS can be produced by XO activation associated with cell death in necrohemorrhagic pancreatitis while the source of ROS in CER-AP is infiltrated neutrophiles[39]. We therefore speculated that pancreatic necrosis is associated with *in situ* increased XO expression. Further analysis of XO alterations in PACs stimulated by various toxins revealed that TLCS, H_2O_2, and ARG were more likely to increase XO activities than cerulein. Consistent findings *in vivo* and *in vitro* studies suggest that the levels of XO expression and enzyme activity are closely correlated with the degree of PACs necrosis and severity.

Given the increased enzyme activity, mRNA, and protein expression of XO were all found after the modeling occurred and most obvious on the inflammatory peak, we sought to determine the therapeutic impact of XOIs on the necrotizing AP model by utilizing two XOIs after the toxic inducer injections. ALLO is a potent purine-like XOI, acting *via* a reversible binding mode with XO. The half-life of ALLO is about 1−2 h; it is quickly oxidized to oxypurinol *in vivo*, which acts as an irreversible covalent inhibitor and has a longer half-life than ALLO[12,40]. FEB, a thiazole derivative, is a highly potent non-competitive inhibitor of XO with an estimated K_i value of around 0.1 nmol/L[41]. *In vitro* molecular docking, cellular thermal shift assay, and PACs necrosis experiments confirmed that XOIs could protect against cell death in PAC. *In vivo*, both ALLO at 30 mg/kg starting from 8 h and FEB at 0.5 mg/kg starting from 48 h showed significant improvement in pancreatic necrosis, although the degree of improvement in other biochemical indicators and remote organs varied slightly. Interestingly, compared with ALLO, which has a relatively weak ability to inhibit XO, FEB requires a lower dose and a shorter dosing time. Therefore, it is speculated that the therapeutic effect of XOIs can only be achieved at appropriate doses and time points to inhibit XO and protect against pancreatic necrosis *in vivo*.

Except for the fact that XO-generated ROS initiated the mitogen-activated protein kinase signaling pathway[25], we do not completely understand how XO functions downstream in necrotic AP. This is the first time to reveal that HIF-1α-regulated metabolic and inflammatory pathways play important roles in the inflammation amplification process after XO activation in AP. It has been reported that XO could activate HIF-1α through oxidative stress in tumor progression[28]. HIF-1α likely regulates NLRP3 inflammasome during acute lung injury[42] and following ischemic stroke[43]. Further, HIF-1α could induce glycolytic reprogramming by increasing the glycolytic protein LDHA[44,45]. In AP, it has been widely accepted that NLRP3 is the main signaling pathway that contributed to severe progression by regulating systematic inflammatory response[46,47]. Inhibition of HIF-1α alleviated acinar cell necrosis[48] and improved intra-pancreatic coagulation[49]. LDH is an indicator of cell death and might distinguish between oedematous and necrotizing pancreatitis[50]. However, the relationship between XO, HIF-1α, and NLRP3 is not clear in AP. Based on the integrated transcriptome and metabolome analyses, NLRP3 and HIF-1α/LDHA signaling pathways were identified in this study. Then we demonstrated that gene and protein expressions of *Hif1a*, *Ldha*, *Nlrp3*, *Il1b*, and *Casp1* in these two pathways changed in the pancreas with XO inhibition or overexpression in animal models. Furthermore, XO/HIF-1α-regulated LDHA/lactate or NLRP3 axis was demonstrated by knockdown of *Xdh* gene in 266-6 cell line or inhibition of XO and HIF-1α on PACs under hypoxia.

red dots for 2 times up-regulation, and pink dots for 1.5 times up-regulation); The bar plot (right) displayed the top 15 metabolites and their correlation coefficients related to urate in comparison AP with Ctrl ($n = 6-9$). (H) The volcano plot (left) showed the differential metabolites between the ALLO *vs*. AP group (green dots for 2 times down-regulation and blue dots for 1.5 times down-regulation); The bar plot (right) displayed the top 15 metabolites and their correlation coefficients related to urate in comparison ALLO with AP. (I) Relative abundances of pancreatic metabolites in glycolysis and purine catabolism. (J) Product/substrate ratios in glycolysis and purine catabolism. Data are presented as mean ± SEM; ns means no significance, $^*P < 0.05$, $^{**}P < 0.01$, and $^{***}P < 0.001$. Abbreviations: FC, fold change; BHB, β-hydroxybutyric acid; F6P/F1P, 1,6-fructose phosphate; G3P, glyceraldehyde 3-phosphate; G6P, glyceraldehyde 6-phosphate; Glu, glucose; Hypoxan, hypoxanthine; Lac, lactate; MDA, malondialdehyde; MNA, methylnicotinamide; N8-AcSPD, *N*8-acetylspermidine; PEP, phosphoenolpyruvic acid; Pyr, pyruvate; TMA, trimethylamine; TMAO, trimethylamine-*N*-oxide; Xan, xanthine.

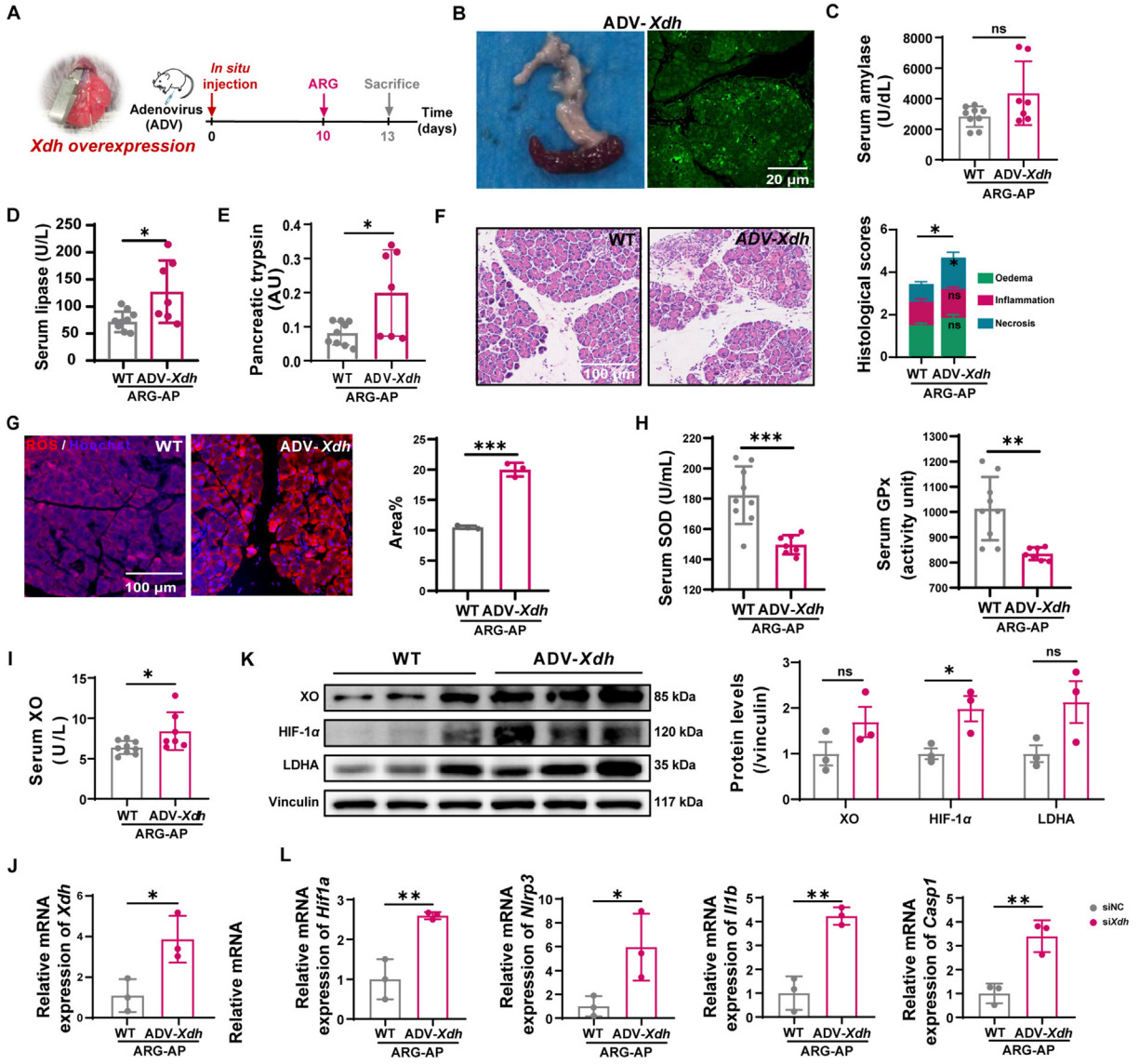

Figure 5 Overexpression of *Xdh* enhanced ARG-AP severity and HIF-1α-mediated LDHA and NLRP3 signaling pathways. (A) The schematic representation of *in situ* injection of pancreas adenovirus and ARG induction. (B) Representative pancreas after adenovirus infection and the expression of green fluorescent protein in adenovirus-transfected pancreas. (C) Serum amylase ($n = 7-9$). (D) Lipase ($n = 7-9$). (E) Pancreatic trypsin ($n = 7-9$). (F) Representative H&E pancreas images with stacked histological scores ($n = 7-9$). (G) Representative images of pancreatic ROS expression in WT-AP and adenovirus-*Xdh* overexpressing AP groups, and their quantitative results on the right ($n = 3$). (H) Serum SOD and GPx activity ($n = 7-9$). (I) Serum XO activity ($n = 7-9$). (J) Relative mRNA expression of *Xdh* ($n = 3$). (K) XO protein expression and quantitative result ($n = 3$). (L) Relative mRNA expression of *Hif1a*, *Nlrp3*, *Il1b*, and *Casp1* in WT-AP and adenovirus-*Xdh* overexpressing groups ($n = 3$). Data are presented as mean ± SEM; ns means no significance, $^*P < 0.05$, $^{**}P < 0.01$, and $^{***}P < 0.001$.

To investigate whether XO activation aggravates severity in AP patients, we examined initial plasma XO activities in three severities of AP patients, as well as pancreatic *in situ* XO gene, protein, and urate levels in SAP patients. We observed a simultaneous elevation of XO enzyme activity in plasma and XO expressions in the pancreas in SAP patients for the first time. These data partly explained the failure of XOI prevention of ERCP-AP in early clinical trials related to not including enough severe patients[17,18,20]. Additionally, since severe pancreatic necrosis or local complications are difficult to identify by computed tomography within the first 72 h after admission[51,52], determining XO levels in the early stages may be recommended for predicting severe cases. Furthermore, the concentrations of lactate and LDH in plasma were significantly higher in the SAP group upon admission, consistent with the findings of Shu et al[53]. Lactate is generally considered a marker of tissue hypoxia and is strongly associated with increased morbidity and mortality in critically ill patients[54]. Hence, lactate accumulation might be associated with XO activation and local hypoxia in SAP patients.

As we mainly focus on whether inhibiting XO alleviates pancreatic damage and its regulated metabolic and inflammatory pathways in SAP, we may underestimate the impact of etiology such as gallstones, alcohol, hypertriglyceridemia, and genetic variation in race, gender, and region on the heterogeneity of the experimental and clinical results[55-57]. Therefore, the main factors in the up-regulation of the *Xdh* gene in SAP remain to be further

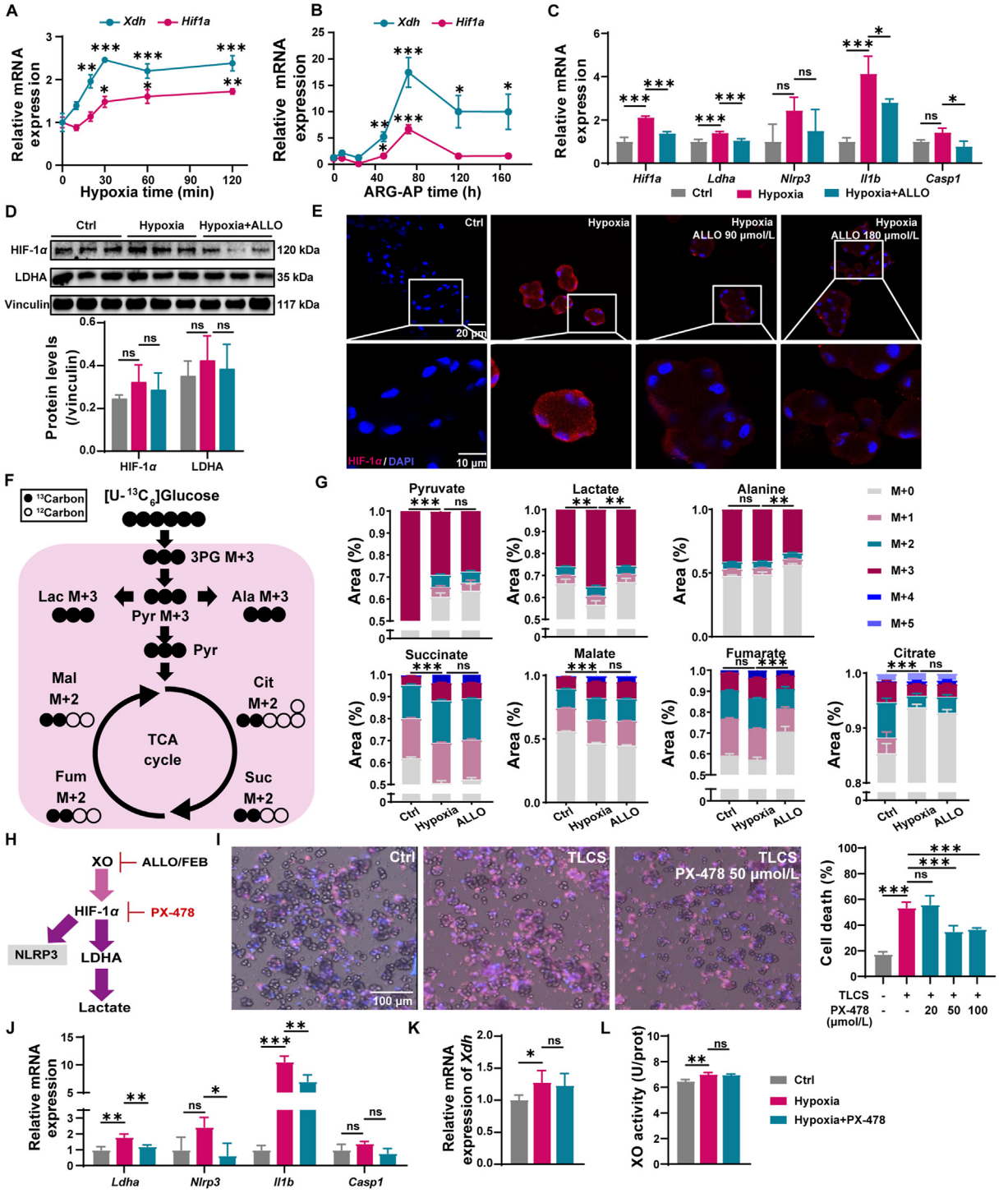

Figure 6 Inhibiting XO down-regulated HIF-1α−LDHA and NLRP3 signal pathways in PACs. (A) Line chart of relative mRNA expressions of *Xdh* and *Hif1a* under hypoxia in PACs at 10, 20, 30, 60, and 120 min ($n = 3$). (B) Line chart of relative mRNA expressions of *Xdh* and *Hif1a* of ARG-AP mice at 8, 24, 48, 72, 120, and 168 h ($n = 6$−11). (C) Relative mRNA expression of *Hif1a*, *Ldha*, *Nlrp3*, *Il1b*, and *Casp1* in ALLO (180 μmol/L) treated PACs ($n = 3$). (D) WB analysis of ALLO-treated PACs ($n = 3$). (E) Representative immunofluorescence images of HIF-1α expression (red) for ALLO intervention at 90 and 180 μmol/L under hypoxia stimulation in PACs. (F) The schematic diagram for the metabolism of [U−^{13}C]-glucose. White circles depict ^{12}C and black solid circles depict ^{13}C. (G) Isotope labeling metabolites in glycolysis and tricarboxylic acid cycle in PACs intervened with ALLO (180 μmol/L) ($n = 3$). (H) A schematic diagram illustrated XO/HIF-1α-regulated NLRP3 and LDHA signaling pathways and their inhibitors. (I) Representative images and quantitative results of cell death induced by TLCS and the protective effect of a HIF-1α inhibitor, PX-478 ($n = 3$). (J) Relative mRNA expressions of *Ldha*, *Nlrp3*, *Il1b*, and *Casp1* in PACs ($n = 3$). (K) Relative mRNA expression of *Xdh* in PACs ($n = 3$). (L) XO activity in PACs ($n = 3$). Data are presented as mean ± SEM; ns means no significance, $^*P < 0.05$, $^{**}P < 0.01$, and $^{***}P < 0.001$. Abbreviations: 3 PG, 3-phosphoglyceric acid; Ala, alanine; Cit, citrate; Fum, fumarate; Lac, lactate; Mal, malate; Pyr, pyruvate; Succ, succinate.

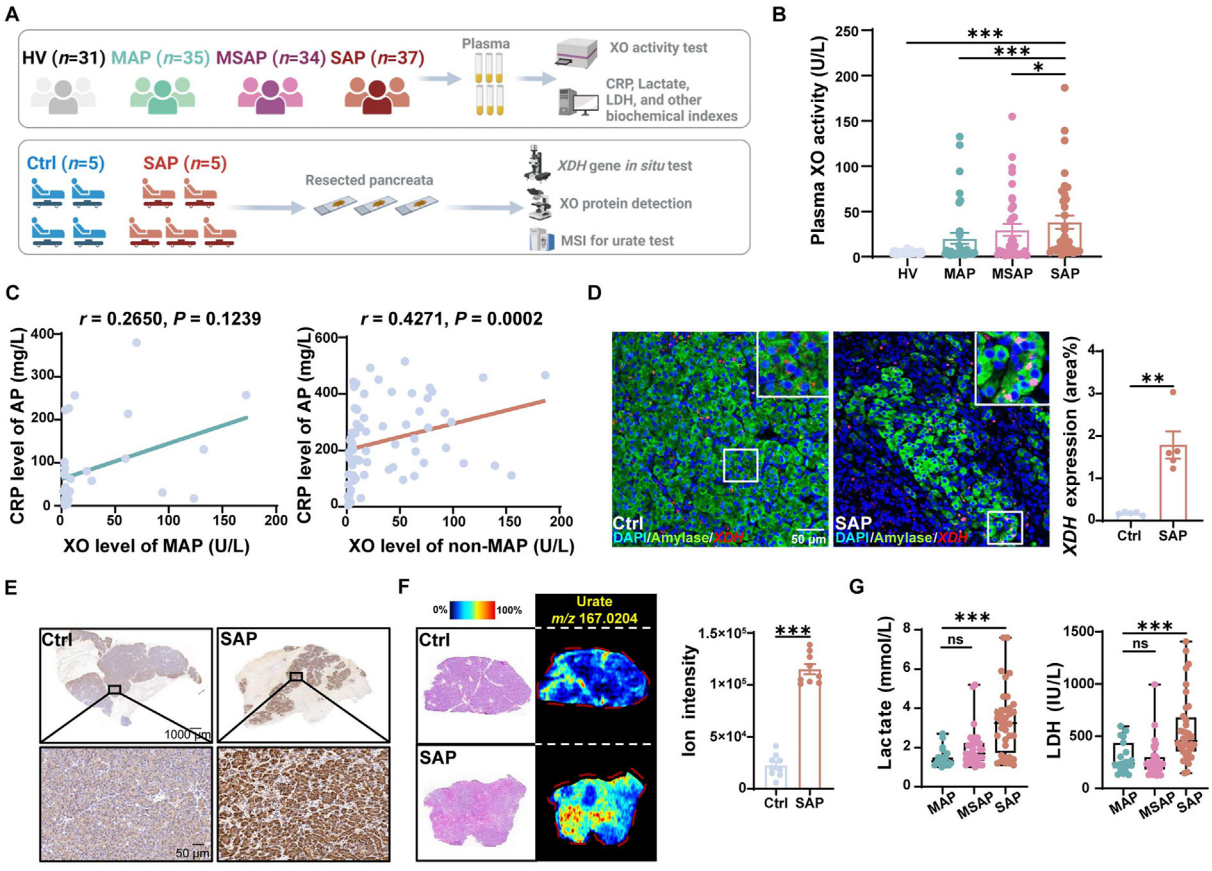

Figure 7 Increased circulative and pancreatic XO in SAP patients. (A) Schematic diagrams of human sample detections. (B) Quantitation analysis of human plasma XO activity (n = 31−37). (C) Correlation analysis between XO and C-reactive protein (CRP) levels in MAP patients (left, n = 35) and non-MAP (MSAP and SAP, right, n = 71) patients. (D) Representative images and quantitative analysis of pancreatic *XDH* gene expression in Ctrl and SAP samples (n = 5). (E) Representative images of pancreatic XO protein expression by IHC. (F) The representative urate distribution in resected human pancreas and quantitative analysis of urate intensities by mass spectrometry imaging (n = 3). (G) Levels of plasma lactate and LDH in MAP, MSAP, and SAP patients on admission (n = 22−36). Data are presented as mean ± SEM, $^{*}P < 0.05$, $^{**}P < 0.01$, and $^{***}P < 0.001$.

explored. Additionally, XO also acts as a metabolic enzyme, catalyzing the final two steps of purine catabolism in humans. Its metabolite, urate, has been reported to be associated with the incidence of SAP[58] and is worthy of further study.

5. Conclusions

In conclusion, increased XO levels were predominantly observed in the peripheral circulation and pancreas of severe necrotizing AP models. Therapeutic inhibition of XO significantly ameliorated PACs necrosis and improved various biochemical indicators of local, circulatory, pancreatic, and remote organ injury to varying degrees. The HIF-1α-regulated LDHA and NLRP3 signaling pathways played important roles in aggravating AP severity. The alterations in XO and its downstream lactate were further identified in SAP patients. Collectively, these findings support the notion that XO is a potential target for aggravating SAP progression, and rational therapeutic doses of XOIs could alleviate severity by modulating HIF-1α-regulated lactate accumulation and the NLRP3 inflammasome pathway.

Acknowledgments

This work was supported by the National Natural Science Foundation of China (Dan Du, 82170905); the Program of Science and Technology Department of Sichuan Province (Dan Du, 2023NSFSC1755, China); the State Key Laboratory of Bioactive Substance and Function of Natural Medicines, Institute of Materia Medica, Chinese Academy of Medical Sciences and Peking Union Medical College (Dan Du, GTZK202107, China); the 1.3.5 Project for Disciplines of Excellence, West China Hospital, Sichuan University (Qing Xia, ZYJC18005, China); and the West China, Nursing Discipline Development Special Fund Project, Sichuan University (Xia Li, HXHL21060, China). The authors thank Qianlun Pu, Yijing Long, Na Jiang, Fei Fu, and Xiyu Wu from the Mass Spectrometry Center for helping with sample preparations; Xiaoting Chen and Guang Yang from the

Experimental Animal Center for help with animal feeding; Xinran Zhou from the Biobank for sample storage and transport; Guonian Zhu from the Institute of Respiratory Health for supporting PCR determinations; Yi Zhang, Wanli Zhang, Yue Li, Jinkui Pi, Liqiang Hu and Sisi Wu from the Research Core Facility as well as Li Li, Fei Chen, and Chunjuan Bao from the Institute of Clinical Pathology of West China Hospital for their help with histopathology examinations. They also appreciate Jiuming He from the State Key Laboratory of Bioactive Substance and Function of Natural Medicines, Institute of Materia Medica, Chinese Academy of Medical Sciences and Peking Union Medical College (Beijing, China) for his help with MSI. They also thank Chengdu Medical College for providing Discovery Studio software, and declare that the graphical abstract was created with BioRender.com.

Author contributions

Juan Rong: Formal analysis, Investigation, Writing − original draft. Chenxia Han: Formal analysis, Investigation, Writing − original draft. Yan Huang: Formal analysis, Investigation. Yiqin Wang: Investigation, Methodology. Qi Qiu: Investigation, Methodology. Manjiangcuo Wang: Data curation, Methodology. Shisheng Wang: Data curation, Methodology. Rui Wang: Investigation, Methodology. Juqin Yang: Data curation, Formal analysis. Xia Li: Resources. Chenggong Hu: Resources. Zhiyao Chen: Resources. Lihui Deng: Resources. Wei Huang: Resources. Qing Xia: Conceptualization, Supervision, Funding acquisition. Dan Du: Conceptualization, Funding acquisition, Writing − original draft, Writing − review & editing.

Conflicts of interest

The authors have no conflicts of interest to declare.

Appendix A. Supporting information

Supporting information to this article can be found online at https://doi.org/10.1016/j.apsb.2024.04.019.

References

1. Mederos MA, Reber HA, Girgis MD. Acute pancreatitis: a review. *JAMA* 2021;**325**:382−90.
2. Lee PJ, Papachristou GI. New insights into acute pancreatitis. *Nat Rev Gastroenterol Hepatol* 2019;**16**:479−96.
3. Leppaniemi A, Tolonen M, Tarasconi A, Segovia-Lohse H, Gamberini E, Kirkpatrick AW, et al. 2019 WSES guidelines for the management of severe acute pancreatitis. *World J Emerg Surg* 2019;**14**:27.
4. Zhang D, Gao M, Jin Q, Ni Y, Zhang J. Updated developments on molecular imaging and therapeutic strategies directed against necrosis. *Acta Pharm Sin B* 2019;**9**:455−68.
5. Rashid MU, Hussain I, Jehanzeb S, Ullah W, Ali S, Jain AG, et al. Pancreatic necrosis: complications and changing trend of treatment. *World J Gastrointest Surg* 2019;**11**:198−217.
6. Werge M, Novovic S, Schmidt PN, Gluud LL. Infection increases mortality in necrotizing pancreatitis: a systematic review and meta-analysis. *Pancreatology* 2016;**16**:698−707.
7. Barreto SG, Habtezion A, Gukovskaya A, Lugea A, Jeon C, Yadav D, et al. Critical thresholds: key to unlocking the door to the prevention and specific treatments for acute pancreatitis. *Gut* 2021;**70**:194−203.
8. Crockett SD, Wani S, Gardner TB, Falck-Ytter Y, Barkun AN. American gastroenterological association institute guideline on initial management of acute pancreatitis. *Gastroenterology* 2018;**154**:1096−101.
9. Moggia E, Koti R, Belgaumkar AP, Fazio F, Pereira SP, Davidson BR, et al. Pharmacological interventions for acute pancreatitis. *Cochrane Database Syst Rev* 2017;**4**:CD011384.
10. Sanfey H, Bulkley GB, Cameron JL. The pathogenesis of acute pancreatitis. the source and role of oxygen-derived free radicals in three different experimental models. *Ann Surg* 1985;**201**:633−9.
11. Sanfey H, Bulkley GB, Cameron JL. The role of oxygen-derived free radicals in the pathogenesis of acute pancreatitis. *Ann Surg* 1984;**200**:405−13.
12. Smelcerovic A, Tomovic K, Smelcerovic Z, Petronijevic Z, Kocic G, Tomasic T, et al. Xanthine oxidase inhibitors beyond allopurinol and febuxostat; an overview and selection of potential leads based on *in silico* calculated physico-chemical properties, predicted pharmacokinetics and toxicity. *Eur J Med Chem* 2017;**135**:491−516.
13. Lankisch PG, Pohl U, Otto J, Wereszczynska-Siemiatkowska U, Gröne HJ. Xanthine oxidase inhibitor in acute experimental pancreatitis in rats and mice. *Pancreas* 1989;**4**:436−40.
14. Hirano T, Manabe T, Ohshio G, Nio Y. Protective effects of combined therapy with a protease inhibitor, ONO 3307, and a xanthine oxidase inhibitor, allopurinol on temporary ischaemic model of pancreatitis in rats. *Nihon Geka Hokan* 1992;**61**:224−33.
15. Czakó L, Takács T, Varga IS, Tiszlavicz L, Hai DQ, Hegyi P, et al. Involvement of oxygen-derived free radicals in L-arginine-induced acute pancreatitis. *Dig Dis Sci* 1998;**43**:1770−7.
16. Czakó L, Takács T, Varga IS, Tiszlavicz L, Hai DQ, Hegyi P, et al. Oxidative stress in distant organs and the effects of allopurinol during experimental acute pancreatitis. *Int J Pancreatol* 2000;**27**:209−16.
17. Budzyńska A, Marek T, Nowak A, Kaczor R, Nowakowska-Dulawa E. A prospective, randomized, placebo-controlled trial of prednisone and allopurinol in the prevention of ERCP-induced pancreatitis. *Endoscopy* 2001;**33**:766−72.
18. Zheng M, Chen Y, Bai J, Xin Y, Pan X, Zhao L. Meta-analysis of prophylactic allopurinol use in post-endoscopic retrograde cholangiopancreatography pancreatitis. *Pancreas* 2008;**37**:247−53.
19. Martinez-Torres H, Rodriguez-Lomeli X, Davalos-Cobian C, Garcia-Correa J, Maldonado-Martinez JM, Medrano-Muñoz F, et al. Oral allopurinol to prevent hyperamylasemia and acute pancreatitis after endoscopic retrograde cholangiopancreatography. *World J Gastroenterol* 2009;**15**:1600−6.
20. Mosler P, Sherman S, Marks J, Watkins JL, Geenen JE, Jamidar P, et al. Oral allopurinol does not prevent the frequency or the severity of post-ERCP pancreatitis. *Gastrointest Endosc* 2005;**62**:245−50.
21. Katsinelos P, Kountouras J, Chatzis J, Christodoulou K, Paroutoglou G, Mimidis K, et al. High-dose allopurinol for prevention of post-ERCP pancreatitis: a prospective randomized double-blind controlled trial. *Gastrointest Endosc* 2005;**61**:407−15.
22. Nordback IH, MacGowan S, Potter JJ, Cameron JL. The role of acetaldehyde in the pathogenesis of acute alcoholic pancreatitis. *Ann Surg* 1991;**214**:671−8.
23. Folch E, Salas A, Panés J, Gelpí E, Roselló-Catafau J, Anderson DC, et al. Role of P-selectin and ICAM-1 in pancreatitis-induced lung inflammation in rats: significance of oxidative stress. *Ann Surg* 1999;**230**:792−8.
24. Folch E, Closa D, Neco P, Solé S, Planas A, Gelpí E, et al. Pancreatitis induces HSP72 in the lung: role of neutrophils and xanthine oxidase. *Biochem Biophys Res Commun* 2000;**273**:1078−83.
25. Pereda J, Sabater L, Cassinello N, Gómez-Cambronero L, Closa D, Folch-Puy E, et al. Effect of simultaneous inhibition of TNF-α production and xanthine oxidase in experimental acute pancreatitis: the role of mitogen activated protein kinases. *Ann Surg* 2004;**240**:108−16.
26. Folch E, Gelpí E, Roselló-Catafau J, Closa D. Free radicals generated by xanthine oxidase mediate pancreatitis-associated organ failure. *Dig Dis Sci* 1998;**43**:2405−10.

27. Bortolotti M, Polito L, Battelli MG, Bolognesi A. Xanthine oxidoreductase: one enzyme for multiple physiological tasks. *Redox Biol* 2021;**41**:101882.
28. Griguer CE, Oliva CR, Kelley EE, Giles GI, Lancaster Jr JR, Gillespie GY. Xanthine oxidase-dependent regulation of hypoxia-inducible factor in cancer cells. *Cancer Res* 2006;**66**:2257−63.
29. de Groot H, Littauer A. Hypoxia, reactive oxygen, and cell injury. *Free Radic Biol Med* 1989;**6**:541−51.
30. Gomez G, Englander EW, Wang G, Greeley GH. Increased expression of hypoxia-inducible factor-1α, p48, and the Notch signaling cascade during acute pancreatitis in mice. *Pancreas* 2004;**28**:58−64.
31. Bai X, Sun B, Pan S, Jiang H, Wang F, Krissansen GW, et al. Down-regulation of hypoxia-inducible factor-1α by hyperbaric oxygen attenuates the severity of acute pancreatitis in rats. *Pancreas* 2009;**38**:515−22.
32. Xiao X, Guo P, Prasadan K, Shiota C, Peirish L, Fischbach S, et al. Pancreatic cell tracing, lineage tagging and targeted genetic manipulations in multiple cell types using pancreatic ductal infusion of adeno-associated viral vectors and/or cell-tagging dyes. *Nat Protoc* 2014;**9**:2719−24.
33. Du W, Liu G, Shi N, Tang D, Ferdek PE, Jakubowska MA, et al. A microRNA checkpoint for Ca^{2+} signaling and overload in acute pancreatitis. *Mol Ther* 2022;**30**:1754−74.
34. Shi N, Liu T, de la Iglesia-Garcia D, Deng L, Jin T, Lan L, et al. Duration of organ failure impacts mortality in acute pancreatitis. *Gut* 2020;**69**:604−5.
35. Banks PA, Bollen TL, Dervenis C, Gooszen HG, Johnson CD, Sarr MG, et al. Classification of acute pancreatitis—2012: revision of the Atlanta classification and definitions by international consensus. *Gut* 2013;**62**:102−11.
36. Fan P, Zhang S, Wang W, Yang Z, Tan W, Li S, et al. The design and implementation of natural population cohort study biobank: a multiple-center project cooperation with medical consortia in Southwest China. *Front Public Health* 2022;**10**:996169.
37. Murphy JA, Criddle DN, Sherwood M, Chvanov M, Mukherjee R, McLaughlin E, et al. Direct activation of cytosolic Ca^{2+} signaling and enzyme secretion by cholecystokinin in human pancreatic acinar cells. *Gastroenterology* 2008;**135**:632−41.
38. Hu Q, Yao J, Wu X, Li J, Li G, Tang W, et al. Emodin attenuates severe acute pancreatitis-associated acute lung injury by suppressing pancreatic exosome-mediated alveolar macrophage activation. *Acta Pharm Sin B* 2022;**12**:3986−4003.
39. Closa D, Bulbena O, Hotter G, Rosello-Catafau J, Fernandez-Cruz L, Gelpi E. Xanthine oxidase activation in cerulein- and taurocholate-induced acute pancreatitis in rats. *Arch Int Physiol Biochim Biophys* 1994;**102**:167−70.
40. Sekine M, Okamoto K, Pai EF, Nagata K, Ichida K, Hille R, et al. Allopurinol and oxypurinol differ in their strength and mechanisms of inhibition of xanthine oxidoreductase. *J Biol Chem* 2023;**299**:105189.
41. Kikuchi H, Fujisaki H, Furuta T, Okamoto K, Leimkuhler S, Nishino T. Different inhibitory potency of febuxostat towards mammalian and bacterial xanthine oxidoreductases: insight from molecular dynamics. *Sci Rep* 2012;**2**:331.
42. Huang JJ, Xia J, Huang LL, Li YC. HIF-1α promotes NLRP3 inflammasome activation in bleomycin-induced acute lung injury. *Mol Med Rep* 2019;**20**:3424−32.
43. Jiang Q, Geng X, Warren J, Eugene Paul Cosky E, Kaura S, Stone C, et al. Hypoxia inducible factor-1α (HIF-1α) mediates NLRP3 inflammasome-dependent-pyroptotic and apoptotic cell death following ischemic stroke. *Neuroscience* 2020;**448**:126−39.
44. Woods PS, Kimmig LM, Sun KA, Meliton AY, Shamaa OR, Tian Y, et al. HIF-1α induces glycolytic reprograming in tissue-resident alveolar macrophages to promote cell survival during acute lung injury. *Elife* 2022;**11**:77457.
45. Masoud GN, Li W. HIF-1α pathway: role, regulation and intervention for cancer therapy. *Acta Pharm Sin B* 2015;**5**:378−89.
46. Sendler M, van den Brandt C, Glaubitz J, Wilden A, Golchert J, Weiss FU, et al. NLRP3 inflammasome regulates development of systemic inflammatory response and compensatory anti-inflammatory response syndromes in mice with acute pancreatitis. *Gastroenterology* 2020;**158**:253−69.
47. Li X, He C, Li N, Ding L, Chen H, Wan J, et al. The interplay between the gut microbiota and NLRP3 activation affects the severity of acute pancreatitis in mice. *Gut Microb* 2020;**11**:1774−89.
48. Shen Q, Shi X, Tao L, Zhu Q, Xiao W, Ding Y, et al. Inhibition of hypoxia-inducible factor-1α alleviates acinar cell necrosis in a mouse model of acute pancreatitis. *Biochem Biophys Res Commun* 2021;**572**:72−9.
49. Park MJ, Iyer S, Xue X, Bragazzi Cunha J, Gu S, Moons D, et al. HIF1-α regulates acinar cell function and response to injury in mouse pancreas. *Gastroenterology* 2018;**154**:1630−4.e3.
50. Komolafe O, Pereira SP, Davidson BR, Gurusamy KS. Serum C-reactive protein, procalcitonin, and lactate dehydrogenase for the diagnosis of pancreatic necrosis. *Cochrane Database Syst Rev* 2017;**4**:CD012645.
51. Balthazar EJ. Acute pancreatitis: assessment of severity with clinical and CT evaluation. *Radiology* 2002;**223**:603−13.
52. Stimac D, Miletic D, Radic M, Krznaric I, Mazur-Grbac M, Perkovic D, et al. The role of nonenhanced magnetic resonance imaging in the early assessment of acute pancreatitis. *Am J Gastroenterol* 2007;**102**:997−1004.
53. Shu W, Wan J, Chen J, He W, Zhu Y, Zeng H, et al. Initially elevated arterial lactate as an independent predictor of poor outcomes in severe acute pancreatitis. *BMC Gastroenterol* 2020;**20**:116.
54. Haas SA, Lange T, Saugel B, Petzoldt M, Fuhrmann V, Metschke M, et al. Severe hyperlactatemia, lactate clearance and mortality in unselected critically ill patients. *Intensive Care Med* 2016;**42**:202−10.
55. Zator Z, Whitcomb DC. Insights into the genetic risk factors for the development of pancreatic disease. *Therap Adv Gastroenterol* 2017;**10**:323−36.
56. Yang AL, Vadhavkar S, Singh G, Omary MB. Epidemiology of alcohol-related liver and pancreatic disease in the United States. *Arch Intern Med* 2008;**168**:649−56.
57. Weiss FU, Laemmerhirt F, Lerch MM. Acute pancreatitis: genetic risk and clinical implications. *J Clin Med* 2021;**10**:190.
58. Su A, Yuan X, Zhu G, Jiang X, Shu R, Yang W, et al. Association between baseline uric acid and the risk of acute pancreatitis: a prospective cohort study. *Pancreas* 2022;**51**:966−71.